Macromolecules

pubs.acs.org/Macromolecules Article

# Kinetic Model for Off-Stoichiometric Cross-Linking Reactions of End-Linked Polymer Networks

Haley K. Beech, Tzyy-Shyang Lin, Hidenobu Mochigase, and Bradley D. Olsen*

Cite This: *Macromolecules* 2023, 56, 9410−9418 Read Online

ACCESS | Metrics & More | Article Recommendations | Supporting Information

**ABSTRACT:** The formation of end-linked polymer networks is commonly modeled as idealized chemical reactions, resulting in defect-free networks. However, many widely used industrial processes including platinum-catalyzed vinyl-silane cross-linking of poly(dimethylsiloxane) (PDMS) are mechanistically complex and involve a variety of side reactions. Here, a kinetic graph theory (KGT) model was updated to account for off-stoichiometric reactive groups and side reactions by adding two fitting parameters representing the relative rate of competing side reactions and the probability of side cross-linking events. The updated KGT outputs the population of each junction type from which the reaction fates of both starting materials are calculated. The elastic effectiveness of the resulting network is calculated with the nonlinear Miller−Macosko theory (MMT), updated to account for side reactions and side cross-linking. The MMT was validated on off-stoichiometric data and was chosen here for its ability to account for a range of effective junction functionalities. Combined, the updated KGT and MMT provide elasticity estimates that capture the experimental peak in elastic modulus observed at an off-stoichiometric silane/alkene ratio in PDMS networks. Both the Lake Thomas and micronetwork fracture theories were subsequently used to estimate the tearing energy, showing a similar peak at off-stoichiometric ratios in qualitative agreement with experimental data. This model is useful in systems where the cross-linking chemistry yields more complex reaction networks, making it relevant to many classes of polymer network chemistry where classical theories may not adequately capture network behavior.

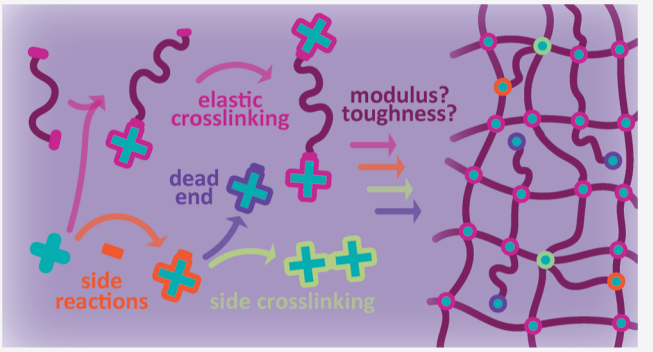




## INTRODUCTION

A longstanding challenge in the field of polymer networks is the accurate prediction of macroscopic properties such as elastic modulus and tearing energy solely on the basis of easily obtainable microscopic information: the starting material chemistry, precursor molecular weight, and polymer volume fraction. Many common industrial polymers employed in network formation are famously messy systems with final properties dependent not only on microscopic details but also on processing conditions such as temperature, reaction atmosphere, and additives.[1−6] Side reactions with impurities such as water or oxygen also impact final properties and can be difficult to control, motivating the use of a model that includes the effects of side reactions. One common example is poly(dimethylsiloxane) (PDMS), which is used for a variety of applications ranging from antifouling and heat-resistant coatings to microfluidic devices to surgical implants.[7−9] Elastic PDMS networks are typically synthesized from bifunctional, vinyl-terminated PDMS cross-linked with *f*-functional silane-containing molecules via a platinum-based catalyst. End-linked PDMS has been studied since the 1970s as a model system for elasticity theories and gelation kinetics.[10−19] Many of these studies employ PDMS cross-linked at a stoichiometric molar ratio $r = \frac{[\text{silane}]}{[\text{vinyl}]} = 1$, despite numerous reports that the optimum mechanical properties are achieved at stoichiometric ratios ranging from $r$ = 1.2−1.75.[10,15,20−23]

Mechanistic and spectroscopic studies provide evidence that the off-stoichiometric peak in properties is due to a variety of side reactions.[10,18,20,24−26] The first mechanism for the platinum-catalyzed vinyl-silane reaction, proposed in the 1960s by Chalk and Harrod, emphasized that platinum is particularly effective at activating both the silane and vinyl group for the reaction.[27] Additional studies have demonstrated that once activated, both the silane and vinyl groups can undergo side reactions with trace oxygen and water molecules in the system, although these are significantly more prevalent among the silane groups.[24−26] Activated silanes react with oxygen or water to create silanol (Si−OH) moieties, which

Received: May 2, 2023
Revised: August 20, 2023
Accepted: October 19, 2023
Published: November 27, 2023

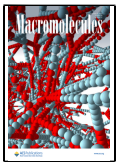

result in a cross-linker of reduced functionality as shown in Figure 1.[26] These silanols subsequently react with other silane

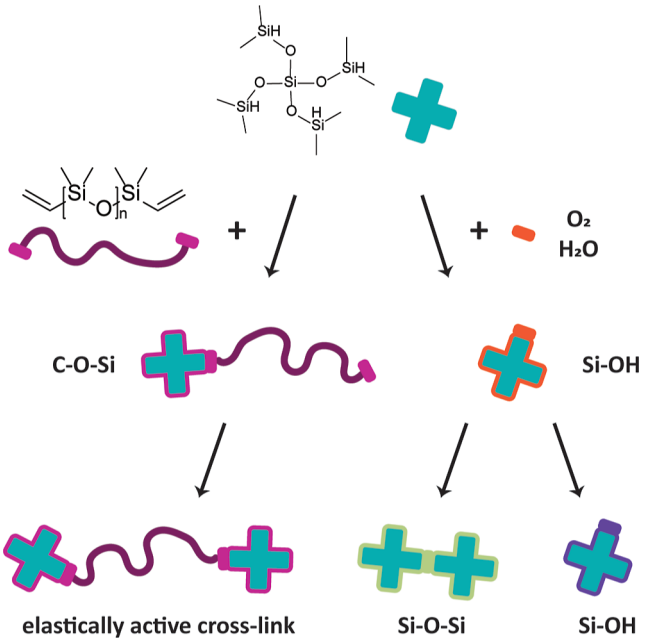


**Figure 1.** Schematic of potential reaction pathways for a silane cross-linker undergoing vinyl-silane chemistry. The silane can react with the vinyl-terminated polymer to create elastically effective bonds (left) or with water or oxygen, resulting in either a dangling silanol group or a side cross-linked Si−O−Si group (right).

or silanol groups to form Si−O−Si bonds, which result in higher-functional cross-linkers. To distinguish these two different types of events, reactions with impurities will be referred to as competing side reactions, while reactions between two cross-links will be referred to as side cross-linking. While these side reactions have been reported to be suppressed when the reaction is run under a dry nitrogen atmosphere,[17,28] this strategy is often inconvenient for practical applications. Furthermore, it has been shown that the platinum catalyst requires trace oxygen to form the proper complex for catalysis, and it is difficult to eliminate all water and impurities from the precursor PDMS due to its high viscosity, creating ample motivation for a model that captures these general classes of side reactions.[24−26]

Current kinetic network generation simulations and elasticity theories typically do not account for the topological heterogeneity created by side reactions. Rate-based theories have been implemented successfully to track loop fractions by Gordon and Temple, Stepto and co-workers, and Lang et al.[29−33] Recently, a kinetic graph theory (KGT) was shown to quantitatively match loop fractions measured experimentally with network disassembly spectrometry.[34−38] KGT is an analytical model that solves a system of differential rate equations that track the kinetics of the formation of an infinitely large network. The rate equations are based on the interconversion of a series of finite subgraphs to complete conversion. In prior work, graph populations were used to calculate loop fractions and the network elasticity based on the elastic effectiveness and starting concentration of material, providing excellent agreement with experimental measurements and kinetic Monte Carlo simulations.[34,36−38]

Here, the KGT method is expanded to encompass polymer networks that contain more complex reaction pathways, including side reactions, using PDMS as a model system. With subgraph populations calculated by the KGT, elastic effectiveness was calculated with an updated version of the nonlinear Miller−Macosko theory (MMT) that accounts for the probability of side cross-linking. Prior work by Gusev et al. has shown that classical MMT theory is readily applicable to PDMS networks when the basic assumptions of equal, independent reactivity and no intramolecular reactions apply.[16,28] MMT was further verified for a set of off-stoichiometric property data and then updated to account for side cross-linking reactions. The KGT + MMT model is compared to data collected on vinyl-silane cross-linked PDMS gels synthesized at a range of stoichiometric ratios and is shown to capture observed trends in mechanical data with two empirical fitting parameters. Tearing energy estimates were made by utilizing elastic effectiveness calculation results. Both classical Lake Thomas theory (LTT) and the micronetwork fracture theory (MFT) were compared to experimental PDMS tearing energy data.[39,40] Quantitative agreement to both elastic effectiveness and tearing energy was obtained by tuning the relative side reaction rate and side cross-linking probability.

## MODEL DETAILS

The structure of networks formed via end-linking of tetra-functional silane molecules ($A_4$) with vinyl-terminated PDMS ($B_2$) is studied with kinetic graph theory. As in the original model developed by Stepto and co-workers,[30,31,41] all reactions are assumed to be kinetically controlled without diffusion limitations, and the assumption of equal reactivity is invoked. First, all of the possible junction species are generated for a given gelation reaction; a subset of the junctions used here is shown in Figure 2 and the complete set is included in Figure S1 in the Supporting Information. Previous single-junction KGT models considered each functional group on a junction to be either dangling (unreacted), connected to a bridging polymer strand, or connected to a looping polymer

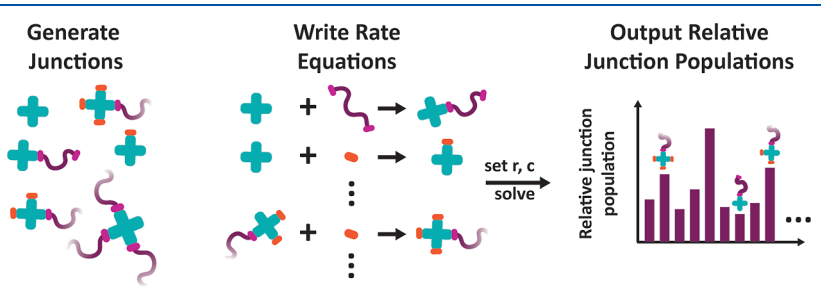


**Figure 2.** Overview of the KGT workflow used to calculate the network topology.



https://doi.org/10.1021/acs.macromol.3c00849
Macromolecules 2023, 56, 9410−9418

strand.[34,36,42] Next, rate equations are written for all possible interconversion pathways between the junction types and solved. Once the system has reached 100% conversion, the number of each type of junction can be counted, and the relative populations of each type are used to capture the topology of the network, as demonstrated in Figure 2. The probability that a given reactive group becomes elastically effective is also calculated to enable the calculation of the mechanical properties. The synthesis concentration and stoichiometry are varied in the KGT to study the effect on the resulting topology and properties.

The KGT model is updated here to include side reactions with impurities. Due to the overlap in elastic effectiveness between two different molecular weight polymers at identical concentrations and stoichiometric ratios, loops are not included in this KGT, although they could easily be accounted for if necessary in a different system. The rates of bridging reactions are calculated with the following rate equation

$$R_{ij,\text{bridge}} = kN_{\text{A},i}N_{\text{B},j}c_ic_j \tag{1}$$

where $k$ is the bimolecular rate constant; $N_{\text{A},i}$ and $N_{\text{B},j}$ are the number of free A and B groups on species $i$ and $j$, respectively; and $c_i$ and $c_j$ are the concentration of species (subgraph) $i$ and $j$, respectively. Competing side reactions with impurities are treated in the KGT with a relative rate parameter, $Y$, labeled on the right side of Figure 3. This parameter is defined as the ratio of the side reactions to bridging reactions as follows

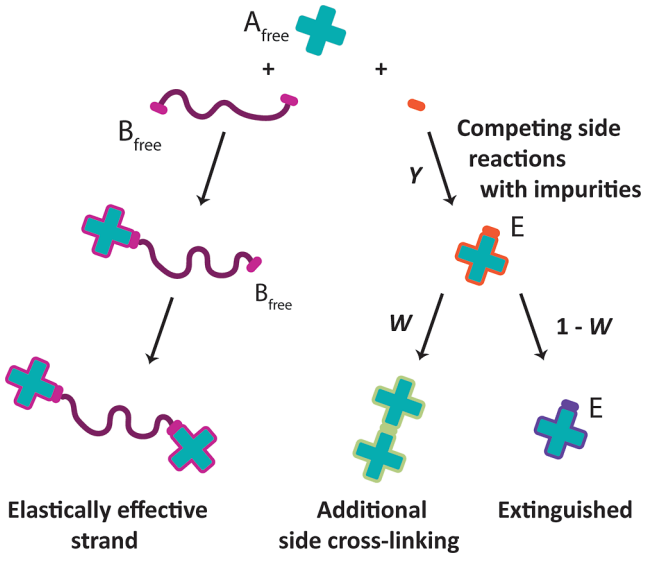


**Figure 3.** Reaction pathways from a free A group include reacting with a free B group (left) or reacting with impurities to extinguish the A group with a relative reaction rate $Y$ (right), which may then side cross-link with a probability of $W$.

$$Y = \frac{R_{i,\text{side}}}{R_{i,\text{bridge}}} = \frac{k_sC_s}{kC_{\text{B},0}} \tag{2}$$

where $k_s$ is the competing reaction rate constant, $C_s$ is the concentration of impurity molecules in the reaction mixture, $k$ is the bimolecular rate constant, and $C_{\text{B},0}$ is the initial concentration of B groups. In a given chemical system, the value of $Y$ could be quantified with independent kinetic studies or estimated with quantum chemical simulation. However, due to the challenges associated with calculating or measuring the rate constants and in situ concentrations of parasitic impurities, they are treated as a fit parameter for the remainder of this analysis. Using the collection of variables defined in eq 2, the rate of competing side reactions is

$$R_{i,\text{side}} = YkN_{\text{A},i}c_iC_{\text{B},0} \tag{3}$$

Solving all of the rate equations for the interconversion between species yields junction populations, which are used to calculate elastic effectiveness of the network. This system of reactions is implemented at the level of a single-junction closure approximation to set boundary conditions for the system.[34,42] A complete representation of the 36 single-junction graphs tracked with a system of 440 differential equations is included in Figure S1 in the Supporting Information. Notably, side cross-linking reactions are not addressed in the KGT; they are instead addressed in the Miller−Macosko calculation of the probability that a given group is not connected to the infinite network. The probability that an extinguished reactive group side cross-links with another E group is defined as $W$ and incorporated into the MMT. This treatment mathematically accounts for these reactions and avoids introducing multijunction species of high functionality in the KGT. The two parameters $Y$ and $W$ are taken as effective fitting parameters for this study, yielding some insight into the likelihood of side reactions that extinguish available reactive groups or side cross-linking in the system based on observed mechanical properties.

The premise of MMT is to first calculate the probability that a given functional group is not connected to the infinite network. This quantity is then the basis for subsequent calculations of physical properties, such as sol fraction or elastic effectiveness. While the full derivation is included in the Supporting Information, it is worth examining two of the basic probabilities which go into the calculation. The probability that a given A group reacts with a B group, $p_{\text{AB}}$ is

$$P(\text{A reacts with B}) = p_{\text{AB}} = 1 - \left(\frac{A_{\text{free}} + E}{A_{\text{tot}}}\right) \tag{4}$$

where $A_{\text{free}}$ is the number of A groups which have not reacted, $E$ is the number of extinguished A groups which have reacted with an impurity, and $A_{\text{tot}}$ is the total number of A groups in the system. Each of these numbers is calculated from the KGT output of the abundance of each type of junction depending on $r$ and the fit parameters $Y$ and $W$. The probabilities of reaction cannot be written as an explicit function of $r$ due to the complex reaction network which is solved numerically (code available on GitHub; see data availability). Following suit, the probability that a given B group reacts with an A group, $p_{\text{BA}}$, is

$$P(\text{B reacts with A}) = p_{\text{BA}} = 1 - \left(\frac{B_{\text{free}}}{B_{\text{tot}}}\right) \tag{5}$$

where $B_{\text{free}}$ is the number of B groups which have not reacted and $B_{\text{tot}}$ is the total number of B groups in the system.

Modulating the relative rate of competing side reactions has a large impact on the probability that A and B groups will react with each other, as opposed to reacting with impurities or extinguished species. As shown in the probability data generated from the KGT output and eqs 4 and 5 in Figure 4, at $r = 1$ and $Y = 0$, $p_{\text{A}} = p_{\text{B}} = 1$; theoretically, all strands should react with cross-linkers to become elastically effective if


https://doi.org/10.1021/acs.macromol.3c00849
Macromolecules 2023, 56, 9410−9418

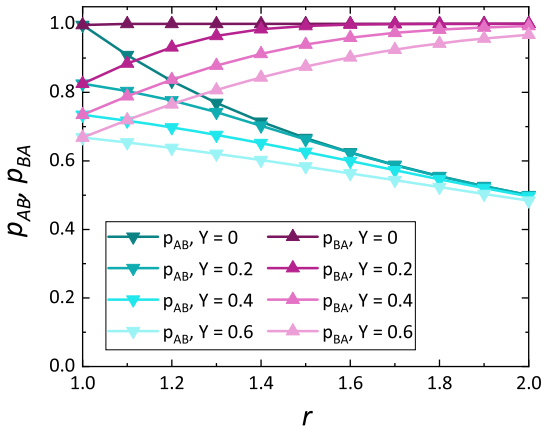


**Figure 4.** Probability that an A group reacts with a B group instead of with an impurity, $p_{AB}$ (blue) compared to the probability that a B group reacts with an A group, instead of remaining free as a dangling end ($p_{AB}$, purple) as a function of stoichiometric ratio, $r$ = A/B, and the relative rate of competing side reactions, $Y$.

there are no side reactions and the reactants are mixed at a stoichiometric ratio. As more cross-linkers are added to the reaction mixture, driving the stoichiometric ratio to values greater than 1, the general trend is a decreased probability that a given cross-linker A will react with a B group, but an increased probability that a given polymer B will react with an A group. This trend becomes stronger as the relative rate of competing side reactions increases. The fraction of polymers that react with cross-linkers is important in determining the final properties of the network, so the increase in $p_{BA}$ at higher $r$ is indicative of a favorable increase in network elasticity at off-stoichiometric ratios.

These probabilities are used in the nonlinear Miller–Macosko theory to iteratively calculate the probability, $P$(A,dis), that a specific reactive group is elastically disconnected, i.e., that it leads to a finite or dangling chain rather than to the infinite network. In the classical theory for an $f$-functional network, the recursive expression is[43]

$$P(\mathrm{A,\ dis}) = p_{\mathrm{AB}} P(\mathrm{A,\ dis})^{f-1} + (1 - p) \tag{6}$$

where $p_{AB}$ is the probability A reacts with B; side reactions are not included in the original derivation. This expression shows good agreement with experimental data on tetra-PEG gels with known reaction efficiencies produced by Akagi et al. as presented in Figures S2 and S3 in the Supporting Information.[44] However, eq 6 needs to be updated to account for the probability that A reacts with an impurity to become extinguished, $E$

$$p_{\mathrm{E}} = \frac{E}{A_{\mathrm{tot}}} \tag{7}$$

where $E$ is the number of extinguished A groups which have reacted with an impurity and $A_{tot}$ is the total number of A groups. The derivation also invokes the probability $W$ that an E group, which has undergone a competitive side reaction, further reacts to create a side cross-link. As such, the probability that a given functional group is not connected to the infinite network in the Miller–Macosko theory, including side reactions and side-cross-linking, is

$$\begin{aligned} P(\mathrm{A,\ dis}) = {} & p_{\mathrm{AB}}[p_{\mathrm{BA}} P(\mathrm{A,\ dis})^{f-1} + (1 - p_{\mathrm{BA}})] \\ & + p_{\mathrm{E}}[WP(\mathrm{A,\ dis})^{f-1} + (1 - W)] \\ & + (1 - p_{\mathrm{AB}} - p_{\mathrm{E}}) \end{aligned} \tag{8}$$

where $P$(A,dis) is the probability that a given reactive group is not connected to the infinite gel molecule and $f$ is the functionality of the junction. The first term corresponds to the probability that a reactive group is not connected to the network given that A reacts with B, the second term corresponds to the probability that a reactive group is not connected to the network given that A reacts to become E, and the final term corresponds to the probability that A does not react. The full derivation for eq 8 is included in the Supporting Information. In the event that $W$ = 0, eq 8 reduces to the original statement of the Miller–Macosko theory, eq 6.

A fundamental network characteristic is the elastic effectiveness, $C$, which represents the deviation from the elastic modulus that would be calculated based on a perfectly elastic, affine network

$$C = G'/\nu_0 k_{\mathrm{b}} T \tag{9}$$

where $G'$ is the elastic shear modulus, $\nu_0$ is the theoretical density of polymer strands, $k_b$ is Boltzmann's constant, and $T$ is the temperature. The total elastic effectiveness is calculated theoretically in this system by counting the fractional elastic effectiveness of each individual chain in the system. This approach is advantageous because it only considers the effective connectivity of chain ends, avoiding the uncertainty inherent to enumerating junction functionality in a system where side cross-linking occurs. There are two types of elastically effective chains in the network, as shown in Figure 5:

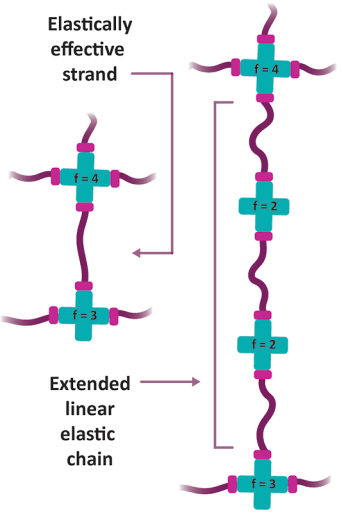


**Figure 5.** Examples of single elastically effective strands (left) and extended linear elastic chains (right).

those that are connected at both ends to network junctions with functionality 3 or higher and those that effectively extend into longer linear chains by virtue of connections with functionality of 2 at one or both ends. In each linearly extended strand containing $n$ chains, there will be $n - 2$ chains with functionality $f$ = 2 at both ends and 2 chains with functionality $f$ = 2 at one end and functionality $f$ = 3 or 4 at the other end. To calculate the effective number of elastically


https://doi.org/10.1021/acs.macromol.3c00849
Macromolecules 2023, 56, 9410–9418

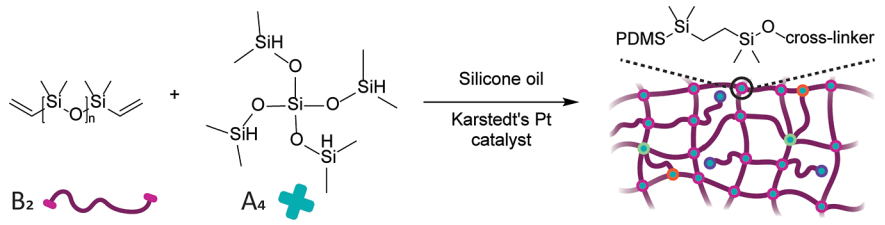


**Figure 6.** Reaction schematic for vinyl-silane PDMS network chemistry.

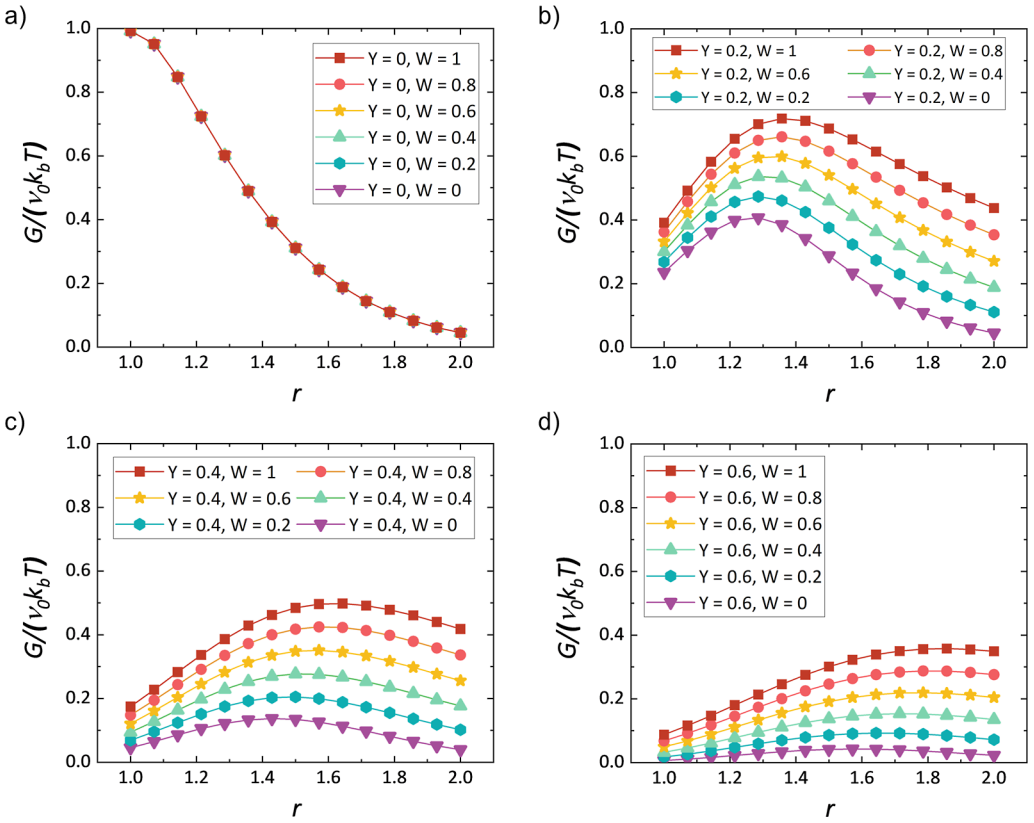


**Figure 7.** Elastic effectiveness as a function of $r$ for competing side reaction relative rates of $Y$ = 0, 0.2, 0.4, and 0.6 [plots (a–d), respectively]; a peak in elastic effectiveness appears at off-stoichiometric ratios when $Y$ is greater than 0. Within each plot, the probability of side cross-linking, $W$, is varied from 0 to 1, which creates a quantitative increase in elastic effectiveness.

effective strands, all strands connected to the gel (junctions of $f$ = 2, 3, 4 at both ends) are denoted as $F_{gel}$. Strands with functionality of $f$ = 2 at both ends, $F_{linear}$, are subtracted as redundant, and each strand with an $f$ = 3 or 4 junction on one end and an $f$ = 2 junction on the other, $F_{partial}$, is counted as half. The total adjustment to elastic strand density is thus the fraction of all strands connected to the gel less the linear strands and half of the partially active strands, as follows

$$C_{eff} = F_{gel} - F_{linear} - \frac{1}{2}F_{partial} \tag{10}$$

Each of these fractional $F$ terms is calculated with the conditional probability of a junction having an effective functionality $f$ given it is connected to the chain of interest; these formulas are dependent on $P$(A,dis) calculated from MMT and are included in the Supporting Information.

The fracture strength of gels and networks is often characterized by the threshold tearing energy, $T_0$, which is the amount of energy per unit area required to propagate a crack across the material.[45−47] LTT was proposed in 1967 to estimate the threshold tearing energy for elastomers[47]

$$T_0 = \frac{1}{2}\nu_0 \bar{L} N U \tag{11}$$

where $\nu_0$ is the overall chain density, $\bar{L}$ is the average displacement length related to the end-to-end distance of the chains, $N$ is the number of segments comprising the strand between the two cross-links, and $U$ is the energy stored in each segment. While the theory captures the qualitative dependence of various parameters on tearing energy, it is known to underestimate the quantitative tearing energy because it neglects effects such as viscoelastic dissipation, polydispersity of precursor strands, and uncertainty in the size of the crack tip.[47,48] The MFT was introduced to account for defects and employs a fracture criterion that considers a crack volume instead of a crack plane, where the fracture occurs when enough strands break to depercolate the network throughout the crack volume. The fracture criterion is thus the percolation threshold


https://doi.org/10.1021/acs.macromol.3c00849
Macromolecules 2023, 56, 9410−9418

$$q \leq \frac{1}{f-1} \tag{12}$$

where $q$ is the fraction of elastically active strands which have not been ruptured. As loops are not considered in this system, the only defects that differentiate the MFT calculation are the impact of longer linear chains such as the one shown on the right in Figure 5.

## EXPERIMENTAL DETAILS

Vinyl-terminated PDMS was reacted with a tetra-functional silane molecule via platinum-catalyzed cross-linking, as illustrated in Figure 6. Vinyl-terminated PDMS with molecular weights of 17.2 and 28 kg/mol was massed in scintillation vials and then diluted with silicone oil to achieve the target volume fraction. Tetrakis(dimethylsiloxy)silane was added to the mixture at varied stoichiometric ratios, and the mixture was stirred until well mixed. Karstedt's catalyst was then added at a concentration of 1−30 ppm and tuned to achieve the desired gelation rate of 1−2 days. The mixture was stirred for an additional 10 min before it was slowly poured or pipetted into a glass mold with a 1 mm polytetrafluoroethylene (PTFE) spacer, lined with PTFE film to allow for easy release. The sample was left to cure for approximately 2 days, after which Fourier transform infrared (FT-IR) spectroscopy was used to confirm complete conversion by the disappearance of silane groups. GPC traces for both prepolymers and representative FT-IR spectra are included in the Supporting Information (Figures S4 and S5).

Rheology was used to measure the elastic shear modulus of the cured networks. Small amplitude oscillatory shear frequency sweeps were conducted on each sample to measure the storage modulus in the linear viscoelasticity regime ($\omega$ = 0.1−100 rad/s, strain = 0.5%). A 10 mm disposable parallel plate geometry was used, with both the top and bottom plates covered with 120 grit sandpaper to prevent slipping. All samples were measured at 25 °C by using a Peltier temperature control stage.

Tearing energy tests were carried out on a Zwick tensile tester using a documented procedure.[40] For each measurement, 3 un-notched and 5 notched samples were cut to dimensions of 30 × 20 × 1 mm. An 8 mm cut was made with a razor blade perpendicular to the short edge on each of the notched samples. Samples were mounted into spring-loaded clamps to obtain a pure shear geometry of 30 mm × 5 mm × 1 mm; the exact thickness, width, and gauge length were measured for each replicate. Samples were pulled at a constant strain of 1 mm/min, and observed to ensure that the crack propagated straight across the sample with no slipping or tearing at the clamps. If necessary, stiffer springs were used to eliminate slipping. Tearing energy was calculated using the Thomas−Rivlin method[46]

$$T_0 = W(\lambda_c)h_0 \tag{13}$$

where $W(\lambda_c)$ is the strain energy per unit volume in the region of the test piece in a state of pure strain at a critical strain, when the crack begins to propagate, is taken to be the point of maximum stress. The initial sample height, $h_0$, is the starting distance between the clamps, taken to be the distance when the sample was under 0.01 N stress at the beginning of the test. The strain energy is calculated by integrating the area under the stress−strain curve of an un-notched sample up to the critical strain value.

## RESULTS AND DISCUSSION

Modulating the values of the side reaction rate $Y$ and the side cross-linking probability $W$ results in a wide range of elastic behavior and captures the appearance of an off-stoichiometric peak. The elastic effectiveness is shown as a function of $r$ for various combinations of $Y$ and $W$ values in Figure 7. When $Y$ = 0 in Figure 6a, in the case of no side reactions, all curves are identical regardless of the value of $W$ and decrease monotonically as a function of $r$, as expected. The quantitative value of $C$ drops to less than 50% of its original value even for the lowest side reaction probability shown at $r$ = 1, indicating that even minimal side reactions will precipitously drop the elasticity of a network prepared under stoichiometric conditions. When $W$ is greater than zero, a peak in the elastic effectiveness is observed and shifts to higher values of $r$ as the probability of side reaction $Y$ increases. When competitive side reactions are present, they cause an effective off-stoichiometric cross-linking at $r$ = 1 by depleting A groups on the cross-linkers, leading to decreased effectiveness. As $r$ increases, more A groups are available, such that side reactions do not deleteriously affect the number of B groups on polymers which react. Changing the value of $W$ shifts the peak position only slightly but has a large impact on the quantitative value of $C$; the ability to react again with an additional cross-linker substantially increases the chance that a given group is connected to the network. This illustrates that it may often be advantageous to operate at an off-stoichiometric ratio in the presence of side reactions rather than attempting to prevent them altogether.

Elastic effectiveness was calculated with the KGT + MMT model and compared to the experimental data. To test the modulus predictions, the model was fit to experimental data collected on 17 and 28 kg/mol PDMS diluted to a polymer volume fraction of 0.24 and reacted at various ratios with a tetra-functional silane cross-linker and Karstedt's catalyst. This dilution was chosen to target the semidilute regime to ensure the gel was not entangled but at a high enough dimensionless concentration where the effect of loops on mechanical properties was minimized, as evidenced by the collapse of two different molecular weights prepared at identical conditions. The elastic modulus of the 17 kDa PDMS network was nearly twice that of the higher molar mass polymer (6.5 ± 0.3 kPa for 28 kDa and 10.6 ± 0.9 kPa for 17 kDa at $r$ = 1.5), as shown in Figure S6 in the Supporting Information. Experimental moduli measurements were converted to elastic effectiveness values by dividing by $\nu_0 k_b T$, with the theoretical $\nu_0$ values for each molecular weight calculated in the Supporting Information. KGT does not track real space positions of the junctions and thus relies on established elasticity theories to predict the mechanical properties, in this case, the MMT.

Moduli at both molecular weights collapse onto one curve in Figure 8 with a peak occurring at $r$ = 1.5, in good agreement with previous reports in the literature.[21,22,49] The best fit of the model occurs at $Y$ = 0.37 and $W$ = 0.31, plotted as a solid line within the error of a majority of the experimental data, especially at $r \geq 1.4$. Physically, this indicates that approximately 37% of the available silane groups undergo competitive reactions with impurities in the system, and of that population, an additional 31% of those extinguished species undergo a side-cross-linking reaction. Although these values are challenging to verify experimentally, they have been reported to vary based on the stoichiometric ratio,[50,51] such that fitting a single, effective value is not likely to perform well across all $r$ values. The close match between data and model in the $r$ = 1.4−2 range suggests that the rate of side reactions may be similar across this entire range and then begin to decrease as the ratio of silane/vinyl groups approaches 1:1.

The same model fit parameters were used to calculate estimates of the tearing energy for data collected on 28 kDa PDMS networks. As shown in Figure 9, Lake Thomas fracture theory fits the data well at $r$ > 1.5, while overestimating at lower $r$. An enhancement factor of 26.1 was used to vertically


https://doi.org/10.1021/acs.macromol.3c00849
Macromolecules 2023, 56, 9410−9418

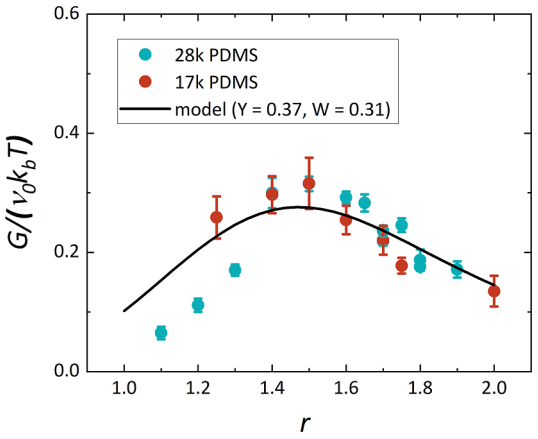


**Figure 8.** Elastic effectiveness calculated from shear modulus measurements for 28 kDa (blue) and 17.2 kDa (red) PDMS prepolymers, compared to the best fit of the KGT + MMT model (black line), with fitting parameters $Y = 0.37$ and $W = 0.31$.

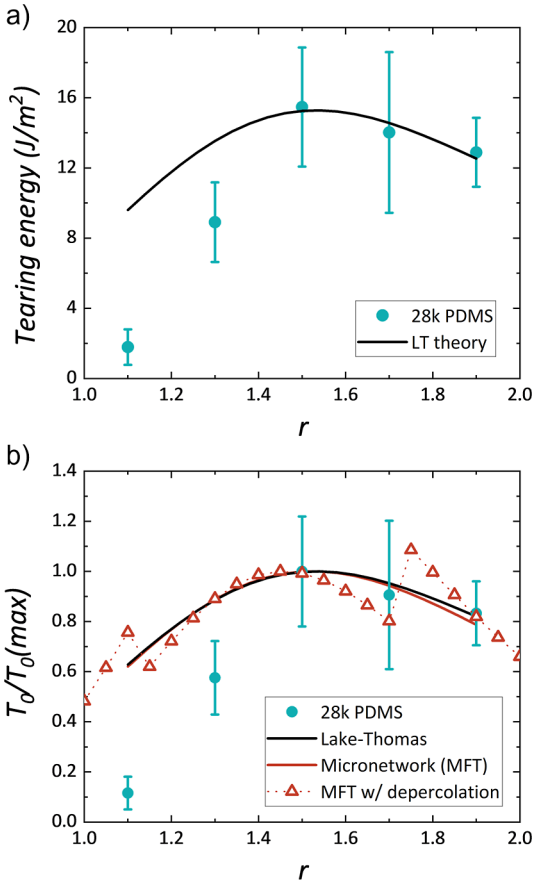


**Figure 9.** (a) Tearing energy measurements (blue circles) and the corresponding LTT fit (black line) were based on the effective elastic effectiveness calculated from the KGT and MMT. (b) Tearing energies normalized to the maximum recorded value with comparisons of the LTT, MFT, and MFT with depercolation theories.

shift the data in Figure 9a, which is reasonable based on reports in the literature of enhancement factors ranging from 3 to over 100.[40,44,52] Similarly to the elastic effectiveness data, the deviation at low $r$ likely corresponds to changing rates of side reactions at smaller excesses of silane.

Tearing energy is normalized with the maximum measured value to compare the LTT to the MFT with and without the depercolation fracture criterion. As shown in Figure 9b, LTT was nearly identical to the results from MFT without the depercolation fracture criteria. Inclusion of the depercolation criterion did not change the values to a degree that would be observable within the error of experimental measurements, especially in light of the relatively high measured dispersity of the PDMS (Figure S4). The step changes in MFT with depercolation correspond to percolation of longer linear strands; these sharp steps are a product of the discrete approach to percolation in the theory and are unlikely to be observed in practical systems. Chain polydispersity and differences in initial conformation, along with the high stochasticity in fracture measurements, make a sharp transition extremely difficult to observe. Gusev et al. found similar agreement in elastic modulus predictions when comparing MMT and an MMT adapted with the Real Elastic Network Theory, likewise due to negligible loop fractions.[16,28] Normalizing all measurements to the maximum recorded value shows a universal trend in mechanical properties as a function of $r$, plotted collectively in Figure S7.

## CONCLUSIONS

A kinetic graph theory was updated to account for competitive side reactions with impurities and the impact of mixing at off-stoichiometric ratios to better predict PDMS property data. Side reactions were added to the KGT with a parameter that captures the relative rate of these competitive reactions compared to the rate of productive bridging reactions. Extinguished reactive groups can further react with each other with a separate probability. This framework, while designed with PDMS in mind, is generalizable to any system with side reactions or off-stoichiometric chemistry. From the reactive probabilities generated by KGT, an updated version of the Miller−Macosko theory was used to calculate the elastic effectiveness of the material, generating usable predictions in good agreement with experimental results. This MMT method is advantageous for this system because it accounts for the many possible complex junction possibilities without explicitly solving for the molecular weight distribution of the junction species. The ability to understand and control the effect that specific side reactions have on final network properties is beneficial for the engineering of industrial elastomers, which often have complex synthetic reaction schemes.

## ASSOCIATED CONTENT

### Data Availability Statement

The Jupyter Notebook code used for the KGT generation and subsequent analysis is available on the Olsen Lab GitHub: https://github.com/olsenlabmit/offstoich_KGT_MMT_model.

### Supporting Information

The Supporting Information is available free of charge at https://pubs.acs.org/doi/10.1021/acs.macromol.3c00849.

Network synthesis and characterization details, derivation of the kinetic graph theory with side reactions, derivation of the revised MMT, elasticity, and tearing energy calculations (PDF)



https://doi.org/10.1021/acs.macromol.3c00849
Macromolecules 2023, 56, 9410−9418

## AUTHOR INFORMATION


### Corresponding Author

**Bradley D. Olsen** − *Department of Chemical Engineering, Massachusetts Institute of Technology, Cambridge, Massachusetts 02139, United States;* orcid.org/0000-0002-7272-7140; Email: bdolsen@mit.edu

### Authors

**Haley K. Beech** − *Department of Chemical Engineering, Massachusetts Institute of Technology, Cambridge, Massachusetts 02139, United States;* orcid.org/0000-0003-3276-8578

**Tzyy-Shyang Lin** − *Department of Chemical Engineering, Massachusetts Institute of Technology, Cambridge, Massachusetts 02139, United States;* orcid.org/0000-0002-8265-6702

**Hidenobu Mochigase** − *Department of Chemical Engineering, Massachusetts Institute of Technology, Cambridge, Massachusetts 02139, United States*

Complete contact information is available at: https://pubs.acs.org/10.1021/acs.macromol.3c00849


### Notes

The authors declare no competing financial interest.

## ACKNOWLEDGMENTS

This work was supported by Dow and the NSF Center for the Chemistry of Molecularly Optimized Networks (MONET), CHE-2116298.

## REFERENCES


(1) Abdilla, A.; D'Ambra, C. A.; Geng, Z.; Shin, J. J.; Czuczola, M.; Goldfeld, D. J.; Biswas, S.; Mecca, J. M.; Swier, S.; Bekemeier, T. D.; Laitar, D. S.; Bates, M. W.; Bates, C. M.; Hawker, C. J. Silicon-Based Polymer Blends: Enhancing Properties Through Compatibilization. *J. Polym. Sci.* **2021**, *59*, 2114−2128.

(2) Miyata, T.; Nakanishi, Y.; Uragami, T. Ethanol Permselectivity of Poly(Dimethylsiloxane) Membranes Controlled by Simple Surface Modifications Using Polymer Additives. *Macromolecules* **1997**, *30* (18), 5563−5565.

(3) Zhang, Y.; Edelbrock, A. N.; Rowan, S. J. Effect of Processing Conditions on the Mechanical Properties of Bio-Inspired Mechanical Gradient Nanocomposites. *Eur. Polym. J.* **2019**, *115*, 107−114.

(4) Calabrese, M. A.; Chan, W. Y.; Av-Ron, S. H. M.; Olsen, B. D. Development of a Rubber Recycling Process Based on a Single-Component Interfacial Adhesive. *ACS Appl. Polym. Mater.* **2021**, *3* (10), 4849−4860.

(5) Madsen, F. B.; Dimitrov, I.; Daugaard, A. E.; Hvilsted, S.; Skov, A. L. Novel Cross-Linkers for PDMS Networks for Controlled and Well Distributed Grafting of Functionalities by Click Chemistry. *Polym. Chem.* **2013**, *4* (5), 1700−1707.

(6) Zhou, J.; Yan, H.; Ren, K.; Dai, W.; Wu, H. Convenient Method for Modifying Poly(Dimethylsiloxane) With Poly(Ethylene Glycol) in Microfluidics. *Anal. Chem.* **2009**, *81* (16), 6627−6632.

(7) Fujii, T. PDMS-Based Microfluidic Devices for Biomedical Applications. *Microelectron. Eng.* **2002**, *61*−*62*, 907−914.

(8) Zhou, J.; Ellis, A. V.; Voelcker, N. H. Recent Developments in PDMS Surface Modification for Microfluidic Devices. *Electrophoresis* **2010**, *31* (1), 2−16.

(9) Klenkler, B. J.; Griffith, M.; Becerril, C.; West-Mays, J. A.; Sheardown, H. EGF-Grafted PDMS Surfaces in Artificial Cornea Applications. *Biomaterials* **2005**, *26* (35), 7286−7296.

(10) Macosko, C. W.; Benjamin, G. S. Modulus of Three and Four Functional Poly(Dimethylsiloxane) Networks. *Pure Appl. Chem.* **1981**, *53* (8), 1505−1518.

(11) Bontems, S. L.; Stein, J.; Zumbrum, M. A. Synthesis and Properties of Monodisperse Polydimethylsiloxane Networks. *J. Polym. Sci., Part A: Polym. Chem.* **1993**, *31* (11), 2697−2710.

(12) Mallam, S.; Horkay, F.; Hecht, A.; Rennie, A. R.; Geissler, E.; Physique, L. D. S.; Fourier, J. Microscopic and Macroscopic Thermodynamic Observations in Swollen Poly(Dimethylsiloxane) Networks. *Macromolecules* **1991**, *24*, 543−548.

(13) Beltzung, M.; Picot, C.; Rempp, P.; Herz, J. Investigation of the Conformation of Elastic Chains in Poly (Dimethylsiloxane) Networks by Small-Angle Neutron Scattering. *Macromolecules* **1982**, *15*, 1594−1600.

(14) Beltzung, M.; Herz, J.; Picot, C. Investigation by Small-Angle Neutron Scattering of the Chain Conformation in Equilibrium-Swollen Poly (Dimethylsiloxane) Networks. *Macromolecules* **1983**, *16* (4), 580−584.

(15) Xu, B.; Wu, J.; McKenna, G. B. Mechanical and Swelling Behaviors of End-Linked PDMS Rubber and Randomly Cross-Linked Polyisoprene. *Macromolecules* **2013**, *46* (5), 2015−2022.

(16) Tsimouri, I. C.; Caseri, W. R.; Gusev, A. A. Monte Carlo Evidence on Simple Conventional Means to Characterize the Final Extent of Reaction of Cured End-Linked Polymer Networks through the Miller-Macosko Nonlinear Polymerization Theory. *Macromolecules* **2021**, *54* (4), 1589−1598.

(17) Chambon, F.; Henning Winter, H. Stopping of Crosslinking Reaction in a PDMS Polymer at the Gel Point. *Polym. Bull.* **1985**, *13*, 499−503.

(18) Kovermann, M.; Saalwächter, K.; Chassé, W. Real-Time Observation of Polymer Network Formation by Liquid- and Solid-State NMR Revealing Multistage Reaction Kinetics. *J. Phys. Chem. B* **2012**, *116* (25), 7566−7574.

(19) Valles, E. M.; Macosko, C. W. Properties of Networks Formed by End Linking of Poly(Dimethylsiloxane). *Macromolecules* **1979**, *12* (4), 673−679.

(20) Sawvel, A. M.; Chinn, S. C.; Gee, M.; Loeb, C. K.; Maiti, A.; Mason, H. E.; Maxwell, R. S.; Lewicki, J. P. Nonideality in Silicone Network Formation via Solvent Swelling and 1 H Double-Quantum NMR. *Macromolecules* **2019**, *52* (2), 410−419.

(21) Genesky, G. D.; Cohen, C. Toughness and Fracture Energy of PDMS Bimodal and Trimodal Networks with Widely Separated Precursor Molar Masses. *Polymer* **2010**, *51* (18), 4152−4159.

(22) Patel, S. K.; Malone, S.; Cohen, C.; Gillmor, J. R.; Colby, R. H. Elastic Modulus and Equilibrium Swelling of Poly(Dimethylsiloxane) Networks. *Macromolecules* **1992**, *25*, 5241−5251.

(23) Macosko, C. W.; Saam, J. C. The Hydrosilylation Cure of Polyisobutene. *Polym. Bull.* **1987**, *18* (5), 463−471.

(24) Stein, J.; Lewis, L. N.; Gao, Y.; Scott, R. A. In Situ Determination of the Active Catalyst in Hydrosilylation Reactions Using Highly Reactive Pt(0) Catalyst Precursors. *J. Am. Chem. Soc.* **1999**, *121* (15), 3693−3703.

(25) Lewis, L. N. On the Mechanism of Metal Colloid Catalyzed Hydrosilylation: Proposed Explanations for Electronic Effects and Oxygen Cocatalysis. *J. Am. Chem. Soc.* **1990**, *112* (16), 5998−6004.

(26) Esteves, A. C. C.; Brokken-Zijp, J.; Laven, J.; Huinink, H. P.; Reuvers, N. J. W.; Van, M. P.; De With, G. Influence of Cross-Linker Concentration on the Cross-Linking of PDMS and the Network Structures Formed. *Polymer* **2009**, *50*, 3955−3966.

(27) Chalk, A. J.; Harrod, J. F. Homogeneous Catalysis. II. The Mechanism of the Hydrosilation of Olefins Catalyzed by Group VII Metal Complexes. *J. Am. Chem. Soc.* **1965**, *87* (1), 16−21.

(28) Tsimouri, I. C.; Schwarz, F.; Caseri, W.; Hine, P. J.; Gusev, A. A. Comparative Experimental and Molecular Simulation Study of the Entropic Viscoelasticity of End-Linked Polymer Networks. *Macromolecules* **2020**, *53* (13), 5371−5380.

(29) Gordon, M.; Temple, W. Ring-Chain Competition Kinetics in Linear Polymers. *Die Makromol. Chem.* **1972**, *152*, 277−289.

(30) Stanford, J. L.; Stepto, R. F. T. Rate theory of irreversible linear random polymrisation. Part 1—Basic theory. *J. Chem. Soc., Faraday Trans. 1* **1975**, *71*, 1292−1307.

(31) Stanford, J. L.; Stepto, R. F. T.; Waywell, D. R. Rate Theory of Irreversible Linear Random Polymerisation. Part 2-Application to Intramolecular Reaction in A-A+ B-B Type Polymerisations. *J. Chem. Soc., Faraday Trans. 1* **1975**, *71*, 1308−1326.
(32) Lang, M. On the Elasticity of Polymer Model Networks Containing Finite Loops. *Macromolecules* **2019**, *52*, 6266−6273.
(33) Lodge, T.; Chapman, B. Applications of Forced Rayleigh Scattering to Diffusion in Polymeric Fluids. *Trends Polym. Sci.* **1997**, *5* (4), 122−128.
(34) Zhou, H.; Woo, J.; Cok, A. M.; Wang, M.; Olsen, B. D.; Johnson, J. A.; Weitz, D. A. Counting Primary Loops in Polymer Gels. *Proc. Natl. Acad. Sci. U.S.A.* **2012**, *109* (47), 19119−19124.
(35) Kawamoto, K.; Zhong, M.; Wang, R.; Olsen, B. D.; Johnson, J. A. Loops versus Branch Functionality in Model Click Hydrogels. *Macromolecules* **2015**, *48*, 8980−8988.
(36) Zhong, M.; Wang, R.; Kawamoto, K.; Olsen, B. D.; Johnson, J. A. Quantifying the Impact of Molecular Defects on Polymer Network Elasticity. *Science* **2016**, *353* (6305), 1264−1268.
(37) Wang, J.; Lin, T.-S.; Gu, Y.; Wang, R.; Olsen, B. D.; Johnson, J. A. Counting Secondary Loops Is Required for Accurate Prediction of End-Linked Polymer Network Elasticity. *ACS Macro Lett.* **2018**, *7* (2), 244−249.
(38) Lin, T.-S.; Wang, R.; Johnson, J. A.; Olsen, B. D. Topological Structure of Networks Formed from Symmetric Four-Arm Precursors. *Macromolecules* **2018**, *51* (3), 1224−1231.
(39) Lake, G. J.; Gent, A. N.; Lindley, P. B. Cut Growth and Fatigue of Rubbers. II. Experiments on a Noncrystallizing Rubber. *J. Appl. Polym. Sci.* **1964**, *8*, 707.
(40) Arora, A.; Lin, T.-S.; Beech, H. K.; Mochigase, H.; Wang, R.; Olsen, B. D. Fracture of Polymer Networks Containing Topological Defects. *Macromolecules* **2020**, *53* (17), 7346−7355.
(41) Dutton, S.; Rolfes, H.; Stepto, R. F. T. Comparison of Ahmad-Rolfes-Stepto Theory, Rate Theory and Monte-Carlo Modelling of Gel Point and Network Modulus. *Polymer* **1994**, *35* (21), 4521−4526.
(42) Zhou, H.; Schön, E. M.; Wang, M.; Glassman, M. J.; Liu, J.; Zhong, M.; Díaz Díaz, D.; Olsen, B. D.; Johnson, J. A. Crossover Experiments Applied to Network Formation Reactions: Improved Strategies for Counting Elastically Inactive Molecular Defects in PEG Gels and Hyperbranched Polymers. *J. Am. Chem. Soc.* **2014**, *136*, 9464−9470.
(43) Miller, D. R.; Macosko, C. W. A New Derivation of Post Gel Properties of Network Polymers. *Macromolecules* **1976**, *9* (2), 206−211.
(44) Akagi, Y.; Sakurai, H.; Gong, J. P.; Chung, U., Il; Sakai, T. Fracture Energy of Polymer Gels with Controlled Network Structures. *J. Chem. Phys.* **2013**, *139* (14), 144905.
(45) Lake, G. J.; Lindley, P. B. The Mechanical Fatigue Limit for Rubber. *J. Appl. Polym. Sci.* **1965**, *9* (4), 1233−1251.
(46) Rivlin, R. S.; Thomas, A. G. Rupture of Rubber. I. Characteristic Energy for Tearing. *J. Polym. Sci.* **1953**, *10* (3), 291−318.
(47) Lake, G. J.; Thomas, A. G. The Strength of Highly Elastic Materials. *Proc. R. Soc. London, Ser. A* **1967**, *300* (1460), 108−119.
(48) De Gennes, P. G. Soft Adhesives. *Langmuir* **1996**, *12* (19), 4497−4500.
(49) Lewicki, J. P.; Harley, S. J.; Finnie, J. A.; Ashmore, M.; Bell, C.; Maxwell, R. S. NMR Investigations of Network Formation and Motional Dynamics in Well-Defined Model Poly(Dimethylsiloxane) Elastomers. *ACS Symp. Ser.* **2013**, *1154*, 133−154.
(50) Quan, X. Properties of Post-cured Siloxane Networks. *Polym. Eng. Sci.* **1989**, *29* (20), 1419−1425.
(51) Gorshov, A.; Kopylov, Y.; Dontsov, A.; Khazen, L. Vulcanization of Methylvinylsiloxane Rubbers with Different Types of Crosslinking Agents. *Introd. Polym. Sci. Technol.* **1986**, *13* (3), T-26.
(52) Okumura, K. Toughness of Double Elastic Networks. *Europhys. Lett.* **2004**, *67* (3), 470−476.


https://doi.org/10.1021/acs.macromol.3c00849
*Macromolecules* 2023, 56, 9410−9418